Research Article | Vol. 7, No. 3 | 1 Mar 2017 | OPTICAL MATERIALS EXPRESS 777

Optical Materials EXPRESS

Substrate-insensitive atomic layer deposition of plasmonic titanium nitride films

ING-SONG YU,[1,6] HSYI-EN CHENG,[2,6] CHUN-CHIEH CHANG,[3] YAN-WEI LIN,[4] HOU-TONG CHEN,[3] YAO-CHIN WANG,[5] AND ZU-PO YANG[4,*]

[1]*Department of Materials Science and Engineering, National Dong Hwa University, Hualien 97401, Taiwan*
[2]*Department of Electro-Optical Engineering, Southern Taiwan University of Science and Technology, Tainan 71005, Taiwan*
[3]*Center for Integrated Nanotechnologies, Los Alamos National Laboratory, Los Alamos, NM 87545, USA*
[4]*Institute of Photonic System, National Chiao Tung University, Tainan 71150, Taiwan*
[5]*Department of Biomedical Engineering, Hungkuang University, Taichung City, 43302, Taiwan*
[6]*Equal contribution*
[*]*zupoyang@nctu.edu.tw*

Abstract: The plasmonic properties of titanium nitride (TiN) films depend on the type of substrate when using typical deposition methods such as sputtering. Here we show atomic layer deposition (ALD) of TiN films with very weak dependence of plasmonic properties on the substrate, which also suggests the prediction and evaluation of plasmonic performance of TiN nanostructures on arbitrary substrates under a given deposition condition. Our results also observe that substrates with more nitrogen-terminated (N-terminated) surfaces will have significant impact on the deposition rate as well as the film plasmonic properties. We further illustrate that the plasmonic properties of ALD TiN films can be tailored by simply adjusting the deposition and/or post-deposition annealing temperatures. Such characteristics and the capability of conformal coating make ALD TiN films on templates ideal for applications that require the fabrication of complex 3D plasmonic nanostructures.

OCIS codes: (160.3918) Metamaterials; (250.5403) Plasmonics; (310.6860) Thin films, optical properties.

References and links

1. Y. C. Yao, Z. P. Yang, J. M. Hwang, Y. L. Chuang, C. C. Lin, J. Y. Haung, C. Y. Chou, J. K. Sheu, M. T. Tsai, and Y. J. Lee, "Enhancing UV-emissions through optical and electronic dual-function tuning of Ag nanoparticles hybridized with n-ZnO nanorods/p-GaN heterojunction light-emitting diodes," Nanoscale **8**(8), 4463–4474 (2016).
2. Y. C. Yao, J. M. Hwang, Z. P. Yang, J. Y. Huang, C. C. Lin, W. C. Shen, C. Y. Chou, M. T. Wang, C. Y. Huang, C. Y. Chen, M. T. Tsai, T. N. Lin, J. L. Shen, and Y. J. Lee, "Enhanced external quantum efficiency in GaN-based vertical-type light-emitting diodes by localized surface plasmons," Sci. Rep. **6**, 22659 (2106).
3. P. Berini and I. D. Leon, "Surface plasmon–polariton amplifiers and lasers," Nat. Photonics **6**(1), 16–24 (2011).
4. A. G. Brolo, "Plasmonics for future biosensors," Nat. Photonics **6**(11), 709–713 (2012).
5. W. Li, U. Guler, N. Kinsey, G. V. Naik, A. Boltasseva, J. Guan, V. M. Shalaev, and A. V. Kildishev, "Refractory Plasmonics with Titanium Nitride: Broadband Metamaterial Absorber," Adv. Mater. **26**(47), 7959–7965 (2014).
6. S. Y. Lin, J. Moreno, and J. G. Fleming, "Three-dimensional photonic-crystal emitter for thermal photovoltaic power generation," Appl. Phys. Lett. **83**(2), 380–382 (2003).
7. N. I. Zheludev and Y. S. Kivshar, "From metamaterials to metadevices," Nat. Mater. **11**(11), 917–924 (2012).
8. G. V. Naik, J. L. Schroeder, X. Ni, A. V. Kildishev, T. D. Sands, and A. Boltasseva, "Titanium nitride as a plasmonic material for visible and near-infrared wavelengths," Opt. Mater. Express **2**(4), 478 (2012).
9. H. E. Cheng and Y. W. Wen, "Correlation between process parameters, microstructure and hardness of titanium nitride films by chemical vapor deposition," Surf. Coat. Tech. **179**(1), 103–109 (2004).
10. J. A. Briggs, G. V. Naik, T. A. Petach, B. K. Baum, D. Goldhaber-Gordon, and J. A. Dionne, "Fully CMOS-compatible titanium nitride nanoantennas," Appl. Phys. Lett. **108**(5), 051110 (2016).
11. H. E. Cheng, W. J. Lee, and C. M. Hsu, "The effect of deposition temperature on the properties of TiN diffusion barriers prepared by atomic layer chemical vapor deposition," Thin Solid Films **485**(1-2), 59–65 (2005).
12. P. Patsalas, N. Kalfagiannis, and S. Kassavetis, "Optical properties and plasmonic performance of titanium nitride," Materials (Basel) **8**(6), 3128–3154 (2015).

#284025 https://doi.org/10.1364/OME.7.000777
Journal © 2017 Received 3 Jan 2017; revised 22 Jan 2017; accepted 31 Jan 2017; published 6 Feb 2017

Optical Materials EXPRESS

13. C. M. Zgrabik and E. L. Hu, "Optimization of sputtered titanium nitride as a tunable metal for plasmonic applications," Opt. Mater. Express **5**(12), 2786 (2015).
14. Y. Wang, A. Capretti, and L. D. Negro, "Wide tuning of the optical and structural properties of alternative plasmonic materials," Opt. Mater. Express **5**(11), 2415 (2015).
15. I. S. Yu, Y. W. Wang, H. E. Cheng, Z. P. Yang, and C. T. Lin, "Surface passivation and antireflection behavior of ALD TiO2 on n-Type silicon for solar cells," Int. J. Photoenergy **2013**, 431614 (2013).
16. Z. P. Yang, H. E. Cheng, I. H. Chang, and I. S. Yu, "Atomic layer deposition TiO2 films and TiO2/SiNx stacks applied for silicon solar cells," Applied Sciences **6**(8), 233 (2016).
17. H. Van Bui, A. W. Groenland, A. A. I. Aarnink, R. A. M. Wolters, J. Schmitz, and A. Y. Kovalgin, "Growth kinetics and oxidation mechanism of ALD TiN thin films monitored by in situ spectroscopic ellipsometry," J. Electrochem. Soc. **158**(3), H214 (2011).
18. H. Kim, "Atomic layer deposition of metal and nitride thin films: Current research efforts and applications for semiconductor device processing," J. Vac. Sci. Technol. B **21**(6), 2231 (2003).
19. E. Langereis, S. B. S. Heil, M. C. M. van de Sanden, and W. M. M. Kessels, "In situ spectroscopic ellipsometry study on the growth of ultrathin TiN films by plasma assisted atomic layer deposition," J. Appl. Phys. **100**(2), 023534 (2006).
20. W. C. Chen, Y. R. Lin, X. J. Guo, and S. T. Wu, "Heteroepitaxial TiN of Very Low Mosaic Spread on Al_2O_3," Jpn. J. Appl. Phys. **42**(1), 208–212 (2003).
21. B. Johansson, J. Sundgren, J. Greene, A. Rockett, and S. Barnett, "Growth and properties of single crystal TiN films deposited by reactive magnetron sputtering," J. Vac. Sci. Technol. A **3**(2), 303–307 (1985).
22. Y. H. Chou, Y. M. Wu, K. B. Hong, B. T. Chou, J. H. Shih, Y. C. Chung, P. Y. Chen, T. R. Lin, C. C. Lin, S. D. Lin, and T. C. Lu, "High-operation-temperature plasmonic nanolasers on single-crystalline aluminum," Nano Lett. **16**(5), 3179–3186 (2016).

1. Introduction

The field of plasmonics and metamaterials has attracted great attention due to their promising properties and applications, such as enhancement of internal quantum efficiency or extraction efficiency for light-emitting devices [1-2], plasmonic lasers [3], plasmonic biosensors [4], broadband metamaterial absorbers [5], thermal emitters [6], etc. These reported nanostructures and metamaterials are typically made of conventional plasmonic materials, e.g., silver (Ag) and gold (Au). However, the high loss at infrared wavelengths has prevented plasmonic nanostructures from achieving optimal performance, and their plasmonic response cannot be easily tuned though it is highly desired for many active device applications. Additionally, these conventional plasmonic materials are incompatible with CMOS technology, and their low melting point also hinders high-temperature applications such as thermal emitters [6].

To address these issues, in the past years a variety of alternative plasmonic materials have been developed, including transparent conducting oxide, e.g., indium tin oxide (ITO), and transition-metal nitrides such as zirconium nitride, hafnium nitride, and titanium nitride (TiN). These materials can exhibit plasmonic response in the visible and infrared regions with higher figure of merit ($-\varepsilon'/\varepsilon''$) as compared to typically used metals and, more importantly, their optical properties can be easily tailored during the deposition process. These properties make them promising materials for plasmonic and metamaterial applications at the visible and near-infrared wavelengths, and further enable active metasurface-based devices [7] allowing for tunable and reconfigurable functionalities. These alternative plasmonic materials also possess other favorable properties, including a much higher melting point and compatibility with Si fabrication processes.

A variety of methods have been employed to deposit alternative plasmonic materials, such as sputtering [8], chemical vapor deposition (CVD) [9], and atomic layer deposition (ALD) [10,11]. Plasmonic properties, for instance in TiN films, have been achieved by sputtering deposition. However, it has been shown that the optical properties of sputtered TiN films are rather sensitive to the underlying substrates [8, 12–14], and an optimization process is needed for different substrates. Recently, CMOS-compatible TiN films were also demonstrated by ALD [10]. Importantly, ALD allows for the fabrication of three-dimensional (3D) plasmonic structures through conformal coating on 3D nanostructured templates of different materials. Therefore, it is of particular importance to investigate the dependence of plasmonic properties of ALD TiN films on substrate materials. Here we show that the substrate material can have a

Optical Materials EXPRESS

very weak impact on the plasmonic properties of the ALD TiN films, and the small variation of plasmonic properties can be compensated simply through controlling the growth temperature or a post-deposition annealing process. Our results also show that particular attention should be paid in ALD to deposit nitride films on the substrates with N-terminated surface.

2. Experiments

ALD of TiN films was carried out using a homemade system described elsewhere [15,16]. We use titanium tetrachloride ($TiCl_4$) and ammonia (NH_3) as precursors and argon (Ar) as purging gas, with a gas flow rate of 32 sccm for NH_3, 40 sccm for Ar, and the flow rate of $TiCl_4$ is controlled by the deposition temperature (here 25 °C). Each deposition cycle includes 8 steps with an equal step duration of 1 second: $TiCl_4$ injection, pumping down, Ar purging, pumping down, NH_3 injection, pumping down, Ar purging, and pumping down. In this study, we use 1000 deposition cycles for all TiN films. Different substrates were cleaned using a standard process and TiN films were deposited together in order to assure the same deposition conditions. Before the deposition, the ALD chamber was pumped down to 5×10^{-2} torr and the growth temperature varies from 450 to 600 °C in different depositions. Post-deposition annealing of TiN films was carried out in vacuum for 1 hour at different temperatures (here 500, 600, and 700 °C). The film optical properties were extracted from ellipsometry measurements (J. A. Woollam Co. α-SE ellipsometer) using Drude-Lorentz model with two Lorentz oscillators [13].

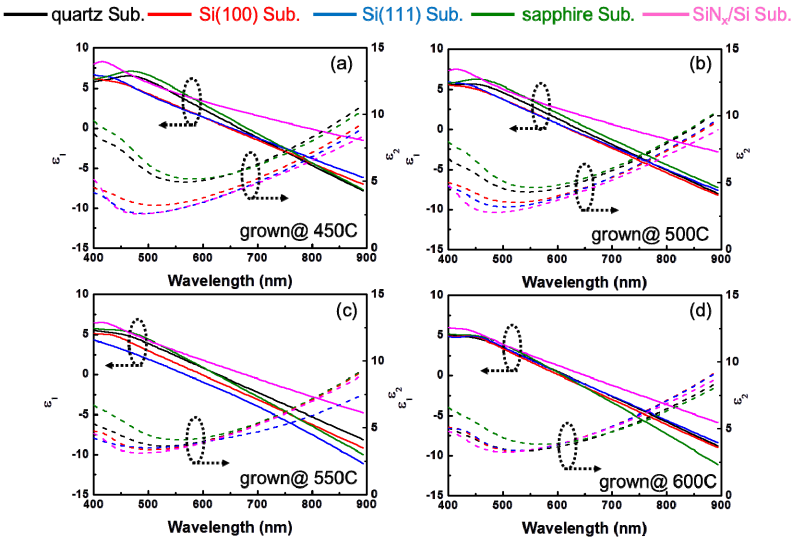

Fig. 1. The extracted complex dielectric function (real part ε_1 and imaginary part ε_2) for ALD TiN films deposited on different substrates at (a) 450 °C, (b) 500 °C, (c) 550 °C, and (d) 600 °C.

3. Results and discussions

Figure 1 shows the extracted complex dielectric function (real part ε_1 and imaginary part ε_2) for TiN films deposited on different substrates and at different temperatures. The extracted values of thickness (Th.) and screened plasmon wavelength (λ_{ps}, where $\varepsilon_1(\lambda_{ps}) = 0$) are summarized in Table 1. These TiN films are all ~20 nm thick, except for those on sapphire and SiN_x/Si substrates, exhibiting a relatively thinner and thicker thickness, respectively, and those deposited at 600 °C, exhibiting increasing thickness. Despite these variations, the deposition rate of 0.02~0.03 nm/cycle agrees with the results reported by other groups [17]. In addition, the deposition rate at 600 °C is relatively faster than those at lower temperatures,

Optical Materials EXPRESS

indicating that the deposition may begin to deviate from the self-limiting growth in our ALD system [18].

Table 1 Summary of extracted thickness (Th.) and screened plasmonic wavelengths (λ_{ps}) of ALD TiN films deposited on different substrates at different deposition temperatures and different post-deposition annealing temperatures.

Growth Temp.	450 °C		500 °C		550 °C		600 °C	
	Th. (nm)	λ_{ps} (nm)	Th. (nm)	λ_{ps} (nm)	Th. (nm)	λ_{ps} (nm)	Th. (nm)	λ_{ps} (nm)
Quartz	16.15	666	19.64	641	23.30	626	33.01	617
Si(100)	20.74	648	21.29	623	22.53	598	32.01	604
Si(111)	21.26	652	21.83	624	22.16	568	35.24	614
Sapphire	13.32	680	14.65	661	17.08	625	21.39	611
SiN_x/Si	33.78	793	33.94	733	35.14	677	45.93	651
Si(100) anneal 500 °C	21.84	626						
Si(100) anneal 600 °C	21.70	596						
Si(100) anneal 700 °C	21.90	563			22.28	548		

All of the ALD deposited TiN films show plasmonic properties, i.e., $\varepsilon_1 < 0$ at wavelengths larger than the screened plasmon wavelength λ_{ps}, which has close values between ~600 nm to ~700 nm except for those films on SiN_x/Si substrates where λ_{ps} is larger. The shortest λ_{ps} of the as-deposited films is obtained when using Si (111) as the substrate and deposited at 550 °C. The extracted $\varepsilon_1(\lambda)$ and $\varepsilon_2(\lambda)$ show similar characteristics in the films deposited on different substrates but at the same temperatures, where the variation of λ_{ps} is less than 40 nm (except for TiN films on SiN_x/Si substrate). This variation is much smaller than those of TiN films deposited by sputtering [8,14], showing ALD deposition can have a relatively weaker substrate dependence than sputtering. It can also be seen from Fig. 1 that, all ALD TiN films deposited at the same temperatures have very similar $\varepsilon_2(\lambda)$, especially for $\lambda > \lambda_{ps}$. It is clear from our results that the substrate material has a very weak impact on both $\varepsilon_1(\lambda)$ and $\varepsilon_2(\lambda)$ of TiN films deposited by ALD. Thus, it becomes possible to predict and evaluate the performance of plasmonic nanostructures on a particular substrate using the plasmonic properties obtained from ALD TiN films on other substrates, which appears to be difficult for sputtering-deposited TiN films.

The deviation of plasmonic properties of TiN films on SiN_x/Si substrates may be associated with the ALD mechanism of TiN deposition. SiN_x/Si substrate has N-terminated surface atoms that $TiCl_4$ molecules look for and then bind with to form Ti-N bond during ALD [18]. Compared with other substrates, more Ti-N bonds will form on SiN_x/Si surface within the first few runs of $TiCl_4$ injections, and NH_3 molecules can then find Ti-covered surface atoms to continue the growth, resulting in a higher deposition rate. This faster deposition seems to be responsible for the relatively large deviation of plasmonic properties of TiN films on SiN_x/Si substrate from other substrates. The dependence of the initial nucleation of ALD TiN films on the surface-terminated atoms was previously investigated by E. Langereis et al [19]. In their study, TiN grown by plasma enhanced ALD was monitored by in situ ellipsometry. They found that TiN nucleation delay is related to the number of reactive surface groups (i.e. hydroxyl groups) on the SiO_2 surface, as the $TiCl_4$ precursor does not react with the siloxane bridges. Besides, for the H-terminated Si surface, an interface layer of SiN_x was formed (due to the exposure of the substrate to the H_2/N_2 plasma) before the nucleation of TiN since $TiCl_4$ molecules are not reactive with H-terminated Si surface but NH_x groups. Their results showed that N-terminated surface can facilitate the TiN nucleation. To confirm the faster ALD growth rate of TiN films on SiN_x/Si substrates, we performed cross-sectional transmission electron microscopy (TEM) for TiN films deposited at 550 °C on

Optical Materials EXPRESS

Si(100) and SiN_x/Si substrates, and the results are shown in Fig. 2(a) and 2(b), respectively. The measured thicknesses of TiN films on Si(100) and SiN_x/Si from TEM images are 23 nm and 37 nm, respectively, which agree well with the ellipsometry results (Table 1). The agreement between ellipsometry and TEM results ensures the accuracy of the extracted complex dielectric function of TiN films from ellipsometry fitting. It can also be seen that TiN films on both substrates show columnar crystalline structures which agrees with the results reported elsewhere [17], although no clear difference (except for film thickness) between these two films is observed in these TEM images. Nevertheless, our analysis and results show that particular attention should be paid in ALD to deposit nitride films on the substrates with N-terminated surface, and more thorough investigations are required in order to further elucidate the underlying physics.

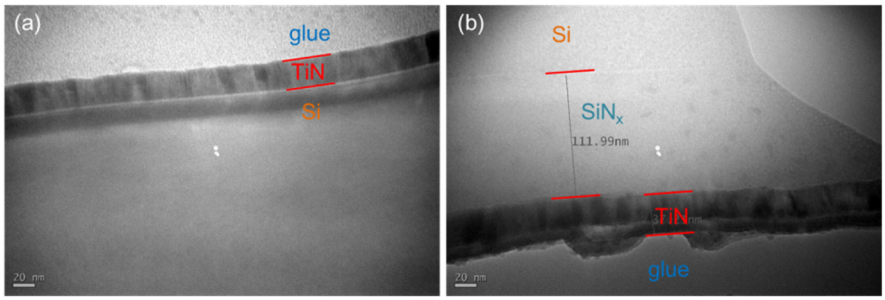

Fig. 2. Cross-sectional TEM images of TiN film deposited at 550 °C on (a) Si(100) and (b) SiNx/Si substrates.

We performed grazing incidence X-ray diffraction (GIXRD) and X-ray diffract (XRD) scans to study the crystallinity of the deposited TiN films on different substrates. Figure 3(a) shows GIXRD results for films deposited at 550 °C. The peaks of TiN(111) and TiN(200) were observed (except for sapphire substrate), indicating polycrystalline characteristic of TiN films. Although from GIXRD results no peak was observed in TiN films on sapphire substrate, XRD scan shown in Fig. 3(b) reveals a strong peak of TiN(111) with fringes, indicating epitaxial growth of TiN films on sapphire substrate [10]. Although not shown here, this peak can be also observed in TiN films deposited at 450 °C on sapphire substrate. These observations can be attributed to the fact that TiN is nearly lattice-matched to sapphire but not to other substrates [20,21]. Though with epitaxial growth, the plasmonic properties of TiN films on sapphire substrates are not much different from those of films on other substrates (except for SiN_x/Si). Similar results were also observed in ALD TiN films on MgO (TiN is nearly lattice-matched to MgO), Si and SiO_2 substrates [10].

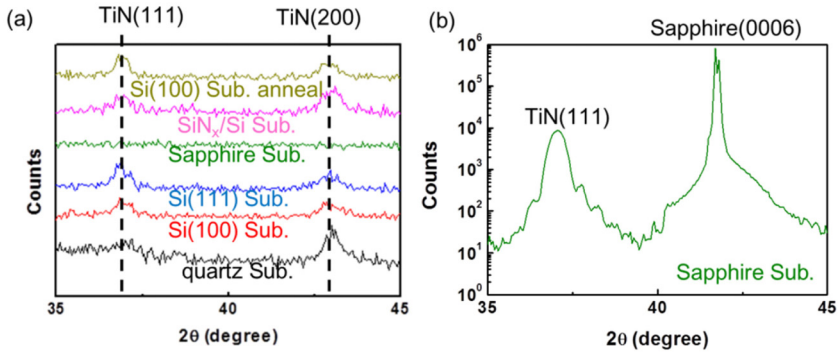

Fig. 3. (a) Grazing incidence X-ray diffraction scan for ALD TiN films deposited at 550 °C on different substrates and the TiN film on Si(100) annealed at 700 °C. (b) X-ray diffraction of ALD TiN film deposited on sapphire at 550 °C.

Optical Materials EXPRESS

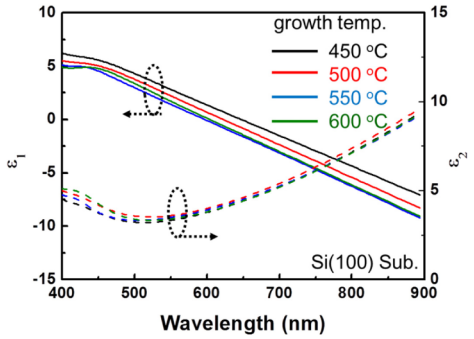

Fig. 4. The extracted $\varepsilon_1(\lambda)$ and $\varepsilon_2(\lambda)$ of ALD TiN films deposited on Si (100) substrates at different temperatures.

It is highly desired to have additional tunability of the TiN plasmonic properties in order to achieve the designed performance of plasmonic nanostructures. Here we show that by simply adjusting the growth temperature and post-deposition annealing we are able to tune the plasmonic properties of ALD TiN films. In Fig. 4 we re-plot the extracted $\varepsilon_1(\lambda)$ and $\varepsilon_2(\lambda)$ of TiN films deposited on Si (100) substrates at different temperatures, which clearly reveals a blue shift of $\varepsilon_1(\lambda)$ (and consequently λ_{ps}) as the deposition temperature increases. For Si (100) and Si (111) substrates the blue shift reaches maximum at 550 °C but it continues on other substrates. For $\varepsilon_2(\lambda)$, there is barely any temperature-dependence observed in films deposited on Si (100) substrates; the deposition temperature-dependence of $\varepsilon_2(\lambda)$ is also very weak when using other substrates. The results demonstrate that the plasmonic properties of ALD TiN films on different substrates can be tuned simply by adjusting the deposition temperature without any significant change of loss.

In Fig. 5(a) and 5(b) we plot the complex dielectric function of TiN films deposited on Si (100) substrates at 450 °C and 550 °C, respectively, after annealed at different temperatures. A clear blue shift can be seen for $\varepsilon_1(\lambda)$ (and consequently λ_{ps}) as the annealing temperature increases. We performed GIXRD scan for the TiN film on Si(100) deposited at 550 °C after annealed at 700 °C (Fig. 3(a)). Both peaks of TiN(111) and TiN(200) become stronger after annealing, indicating the enhanced TiN crystallinity after annealing. Y. Wang et al. also observed the blue shift of λ_{ps} of sputtered TiN films with increasing annealing temperature, and the blue shift was attributed to the expansion of crystalline size [14]. Again, $\varepsilon_2(\lambda)$ remains basically unchanged upon different annealing temperatures. Compared with tuning by varying the deposition temperature, post-deposition annealing can result in larger blue shifts, thus providing a promising and additional route to tune the plasmonic response of ALD TiN films deposited on different substrates.

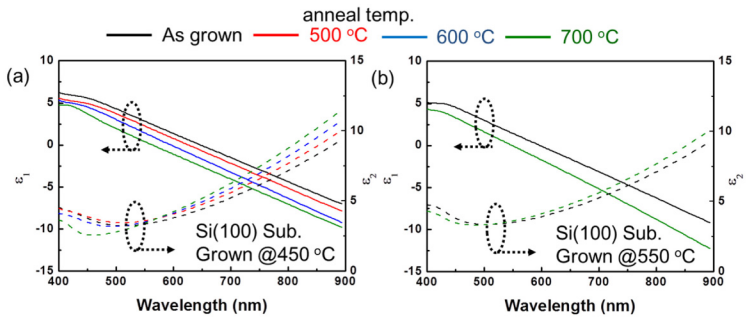

Fig. 5. $\varepsilon_1(\lambda)$ and $\varepsilon_2(\lambda)$ for ALD TiN films deposited on Si (100) substrates at (a) 450 °C and (b) 550 °C, after post-deposition annealing at different temperatures.

Optical Materials EXPRESS

Since the surface roughness scattering is one of the venues contributing to the plasmonic loss and the main limiting factor for achieving plasmonic laser operated at high temperatures [22], we performed atomic force microscopy (AFM) for the TiN films on Si(100) deposited at 450 °C and the films annealed at 500 °C – 700 °C (Fig. 6). The root mean square roughness for the as-deposited and annealed at 500 °C, 600 °C, and 700 °C TiN films are 0.195 nm, 0.206 nm, 0.323 nm, and 0.198 nm, respectively. These results reveal that the ALD TiN films have atomically smooth surface resulted from the intrinsic deposition mechanism of ALD. The annealed TiN films have similar surface roughness as as-deposited TiN films, indicating that the thermal annealing does not deteriorate the surface of ALD TiN films and hence is a feasible method to tune the plasmonic properties of ALD TiN films.

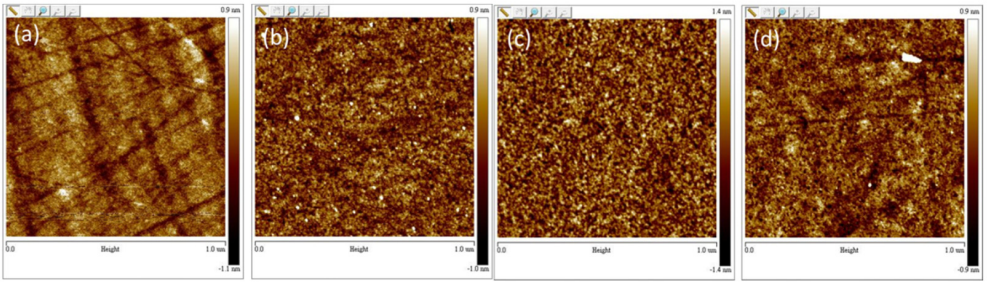

Fig. 6. AFM images for the TiN films on Si(100) deposited at 450 °C. (a) as-deposit, (b)-(d) annealed at 500 °C, 600 °C, and 700 °C, respectively.

Finally, we show that ALD can be used to deposit conformal coating of TiN films on 3D nanostructures with a high aspect ratio, which can serve as the template for the fabrication of 3D TiN-based complex plasmonic nanostructures. To this end, we first fabricated anodic alumina oxide (AAO) templates on Si substrates with an aspect ratio of ~10, defined by the ratio of AAO hole diameter to hole depth. ALD TiN films were then deposited at 550 °C, with the cross-sectional scanning electron microscopy (SEM) image shown in Fig. 7, which clearly reveals the TiN film of a thickness of ~30 nm that was conformally coated on the walls of holes within the entire AAO matrix, suggesting the feasibility of ALD fabrication of 3D TiN-based complex plasmonic nanostructures.

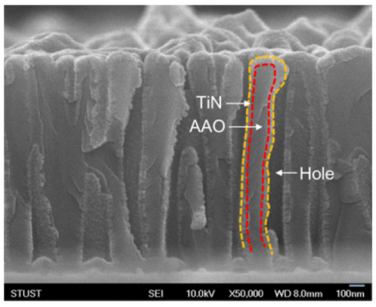

Fig. 7. Cross-sectional SEM image of ALD TiN-coated AAO template. Red dashed line indicates the AAO surface, and yellow dashed line the TiN surface after deposition.

4. Conclusions

In summary, we show the weak substrate dependence of plasmonic properties in ALD TiN films on different substrates. Our results suggests that the plasmonic properties obtained from ALD TiN films on one substrate can be used to predict and evaluate the plasmonic performance of TiN nanostructures on other substrates, which appears to be difficult for films deposited by other commonly used methods, e.g., sputtering. It was also shown that substrates with N-terminated surface will significantly increase the TiN film deposition rate and

Optical Materials EXPRESS

consequently affect the plasmonic properties. We further show that the plasmonic properties of ALD TiN films can be effectively tuned, by simply adjusting the deposition temperature and performing post-deposition annealing. The capability of ALD conformal coating of plasmonic TiN films paves a promising avenue for fabricating complex 3D TiN-based plasmonic nanostructures and metamaterials for a host of applications.

Funding

The authors gratefully acknowledge the financial support from Ministry of Science and Technology (contract no. MOST 105-2221-E-009-073, 105-2221-E-259-003, and 105-2221-E-218-001). This work was partially supported by LANL LDRD program, and performed, in part, at the Center for Integrated Nanotechnologies, a U.S. Department of Energy, Office of Basic Energy Sciences Nanoscale Science Research Center operated jointly by Los Alamos and Sandia National Laboratories. The authors also would like to thank Mr. Lee of National Cheng Kung University for the support of X-ray diffraction scan.